PAPER

Check for updates

Generation of hydrogen sulfide during the thermal enhanced oil recovery process under superheated steam conditions

Qiang Ma,†[ab] Zhengda Yang,†[a] Liqiang Zhang,[a] Riyi Lin*[a] and Xinwei Wang[a]

During the thermal enhanced oil recovery (EOR) process, the hazardous hydrogen sulfide (H_2S) gas among the produced gases causes significant difficulty in the exploration and development of petroleum. In this study, the effects of superheat degree on the H_2S generation by heavy oil aquathermolysis were explored through simulated experiments. The crude and residual oils before and after the reaction were separated into saturate, aromatic, resin and asphaltene fractions (SARA). The oil samples were analyzed from various perspectives by various characterization methods including Fourier transform infrared (FTIR) spectroscopy, elemental analysis, and X-ray photoelectron spectroscopy (XPS). The results showed that H_2S generation was favored by larger superheat degree at the same temperature, and it increased from 0.178 to 0.345 mL g^{-1} oil with an increase in the superheat degree from 62.19 to 89.42 °C. The contents of the sulfur-containing substances, which were supposed to be the main sources of H_2S generation, in the saturate and aromatic fractions decreased significantly with an increase in the superheat degree; the increase in the superheat degree led to a slight reduction in the contents of the methylene, methyl and carboxyl/carbonyl groups. Moreover, the analysis of the main sulfur existing forms before and after the reaction suggests that sulfur in the forms of sulfides, sulfones and sulfates is more likely to generate H_2S under superheated steam conditions. This study provides an understanding of the mechanism of H_2S generation during the process of injecting superheated steam for heavy oil recovery.

1. Introduction

In recent years, the exploitation of high-viscosity heavy oil has attracted extensive attention due to the reduction of conventional oil reserves.[1–3] Steam-assisted oil recovery is one of the most effective technologies to develop heavy oil reservoirs.[4–6] Complex chemical reactions occur during the steam injection process. Consequently, not only the physical properties of heavy oil will change, but also some hazardous gases will be generated.[7] In particular, hydrogen sulfide (H_2S) at extremely high concentrations has been observed in some oil fields, which threatens the safety of production equipment and workers.[8]

Currently, it has been pointed out that H_2S is generated through aquathermolysis reactions.[9] However, aquathermolysis is a very complex reaction, and the production mechanism of H_2S is not fully understood.[7] Hyne *et al.* first carried out the aquathermolysis test using two heavy oil samples at 200–300 °C.[10] During the steam injection process, the condensation, ring-opening, hydrodesulphurization, and water gas shift reactions occurred between steam and heavy oil; the composition of the gas obtained from the heavy oil reaction was the same as that of the gas obtained from sulfur-containing model compounds such as thiophene and thiolane. The aquathermolysis reaction is very complicated such that a number of aquathermolysis experiments have been conducted to investigate the influencing factors for H_2S generation *via* the aquathermolysis of heavy oil. Na *et al.* carried out aquathermolysis tests with bitumen samples in an H_2S corrosion-resistant autoclave, and the gas composition after each reaction was analyzed, the results of which showed that the amounts of H_2S and CO_2 increased with an increase in the reaction time and temperature.[11] Montgomery *et al.* separated the heavy oil into saturate, aromatic, resin and asphaltene fractions (SARA) and found that the H_2S generation could be minimized using specific temperature and pressure.[12,13] Moreover, some researchers have revealed that H_2S generation can be promoted by the catalytic effect of minerals. The H_2S concentration was higher when minerals were present in the aquathermolysis reaction mixture,[14,15] and the reaction temperature of aquathermolysis could be reduced due to this catalytic effect.

The reaction temperature can influence the water status, and some researchers have explored the role of water status,[16–18] water dielectric constant[19] and solubility[20,21] in H_2S generation. The results showed that water participated in the aquathermolysis reaction simultaneously as a catalyst, reactant and solvent. The

[a]College of New Energy, China University of Petroleum (East China), Qingdao 266580, P. R. China. E-mail: linry@upc.edu.cn; Tel: +86-0532-8698-1767

[b]China Petroleum Pipeline Engineering Co., Ltd, Langfang, Hebei, 100044, China

† Equal contribution author.

This journal is © The Royal Society of Chemistry 2019

dissociation constant of water increased by three orders of magnitude at 200 °C, and consequently, water showed the catalytic effect of acid, alkali or acid–alkali double catalysts in the reaction process. The generation of H_2S increased with a decrease in the pH value when the heavy oil reacted with water.[22]

Recently, the utilization of superheated steam for heavy oil recovery has gained extensive attention because superheated steam carries more energy as compared to saturated steam. However, the heat transfer characteristics of the two-phase flow in micro-channels can be significantly different.[23] Sun et al. investigated the flow and heat transfer characteristics of superheated steam in steam injection wells.[24,25] The distributions of pressure and temperature of superheated steam in multi-point injection horizontal wells could be predicted using a numerical model, and it was found that the wellbore heat efficiency increased with the increasing superheat degree.[26] Compared with heavy oil recovery by conventional steam, the oil recovery was proven to be significantly improved by superheated steam.[23] However, the mechanism of the aquathermolysis reaction and corresponding H_2S generation under superheated steam conditions has not been well understood to date.

This study focused on the effects of superheat degree on the H_2S generation during a simulated thermal enhanced oil

recovery process. The superheat degree of steam was well-controlled by changing the reaction temperature and pressure. The mechanism of H_2S generation was revealed by analyzing the gas composition, elemental contents, structure and functional groups of the heavy oil before and after the reactions. This study provides an insight into the mechanism of H_2S generation and may help to analyze the possible H_2S generation using superheated steam during the thermal enhanced oil recovery process in the future.

2. Materials and methods

2.1 Oil sample

In this study, the tested heavy oil was obtained from the Liaohe Oil Field. To identify the main sources of H_2S generation, the oil sample was separated into saturate, aromatic, resin and asphaltene fractions according to the China Petroleum NB/SH/T 0509-2010. The elemental contents of both original heavy oil and SARA were measured by an elemental analyzer (Vario EL III, Elementar, Germany). The SARA fractions and elemental contents are presented in Table 1. The heavy oil sample was low-sulfur crude oil because the overall sulfur content was as low as 0.45%. The main fraction was the resin fraction that accounted for 44.28% of the total fractions, which led to the high viscosity of heavy oil; the sulfur content was significantly high in the aromatic fraction than in other fractions.

2.2 Apparatus and procedures

As depicted in Fig. 1, the experimental setup mainly consists of the aquathermolysis reactor, a temperature and pressure control system, and a gas detection system. The reactor was a stainless steel autoclave, which was designed to operate at a maximum temperature of 600 °C and a maximum pressure of 20 MPa. Since

Table 1 SARA and elemental contents of heavy oil

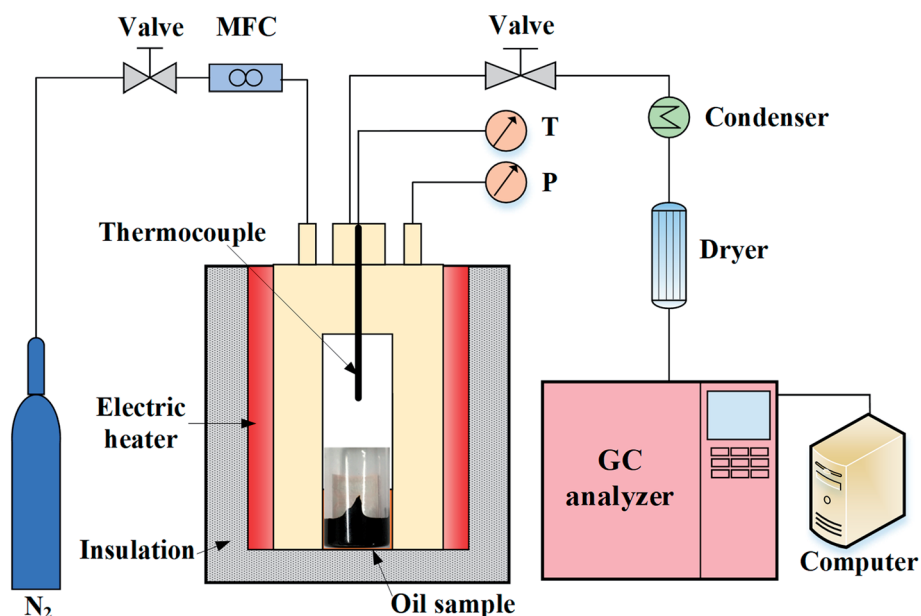|	Contents (%)	Element contents (%)				
		H	C	N	S	Others
Crude oil	100	11.04	85.18	0.97	0.45	2.36
Saturate	25.43	12.01	85.08	0.00	0.12	2.79
Aromatic	21.08	10.68	84.11	0.51	0.78	3.92
Resin	44.28	11.15	86.26	1.62	0.48	0.49
Asphaltene	9.21	8.68	82.74	1.60	0.43	6.55

Fig. 1 Schematic of the experimental setup.

the volume of a single autoclave is fixed, four autoclaves with different volumes (320, 380, 440 and 500 mL) have been utilized in this study. To avoid reactions between heavy oil and metal, the samples (3.0 g oil and 10 mL deionized water) were loaded onto a quartz glass cylinder encapsulated in the autoclave. The autoclave reactor was heated by an electrically tubular furnace, which enabled the temperature of the reactor to increase from ambient temperature to reaction temperature within 5 min. The temperature was measured and monitored by a K-type thermocouple placed in the center of the quartz glass cylinder. At the beginning of each experiment, nitrogen was repeatedly filled into the reactor to remove the air inside the reactor. After carefully checking the gas tightness, the autoclave was pressurized to 10 MPa at ambient temperature. In this study, the superheat degree was investigated at the temperatures of 200, 250 and 300 °C. After reaction for 24 h, the reactor was cooled down to ambient temperature. Both the gas products and oil were obtained after the reaction for further analysis.

The gas products were dried by a drying cylinder prior to detection. The H_2S concentration was measured by an on-line H_2S detector (AKRT-H_2S-W, AKRT, USA). The other gases were obtained by a gas sampling bag at ambient temperature and then analyzed by gas chromatography (7890A, Agilent, USA). The residual oil and the separated SARA were analyzed by an elemental analysis, Fourier transform infrared spectroscopy (FTIR 870, NEXUS, USA) and X-ray photoelectron spectroscopy (XPS, ESCALab-250Xi, ThermoFisher, USA). The FTIR spectroscopy was utilized to characterize the functional groups containing heteroatoms in heavy oil. The oil samples were prepared for the FTIR tests by homogenizing 1 mg of oil with 100 mg of potassium bromide. XPS was utilized to characterize the existing form of heteroatoms in heavy oil. The oil samples were spread on a slide of 5 mm × 5 mm and dried in a drying oven for 2 hours for the XPS tests. The elemental peaks were fitted using the software XPSPEAK41.

2.3 Determination of superheat degree

The status of superheated steam can be determined by a set of parameters including temperature and pressure. At the same temperature, the gas pressure can be changed by adjusting the reactor volume. However, the reactor volume was immutable in this study. To obtain various pressures, four autoclaves with different volumes were utilized, and the temperature and water amount were kept constant. The exact partial pressure of steam can be calculated according to the Dalton's law of partial pressure. The saturation temperature (T_s) corresponding to the partial pressure can refer to the thermodynamic steam property. Finally, the superheat degree (ΔT) can be determined by ($T - T_s$). In this study, the superheat steam was investigated at three temperatures (200, 250, and 300 °C), and the superheat degrees obtained at 250 °C, as an example, are listed in Table 2.

3. Results and discussion

3.1 Gas generation under superheated steam conditions

The aquathermolysis reaction is very complicated such that various gas products can be detected after each experiment. The

Table 2 Calculation of the superheat degree at 250 °C

No.	t (h)	T (°C)	P (MPa)	T_s (°C)	ΔT (°C)
Case 1	24	250	2.62	226.46	23.54
Case 2	24	250	2.07	214.12	35.88
Case 3	24	250	1.71	204.59	45.41
Case 4	24	250	1.57	200.46	49.54

gas compositions after reactions at the four superheat degrees obtained at 250 °C are listed as an example in Table 3. Organic gases such as CH_4, C_2H_6, C_2H_4, C_2H_4 and C_4H_{10} accounted for the majority of the total gases. Moreover, inorganic gases such as H_2, CO_2 and H_2S were detected. Although the amounts of the inorganic gases were much lower than those of the organic gases, their significance in the characterization of the aquathermolysis reaction could not be ignored.

The generation of H_2 during the aquathermolysis reaction might be due to the water gas reforming reaction.[17,27,28] Hydrogen has the ability to rapidly capture hydrocarbon radicals, which can effectively inhibit the polycondensation reaction during aquathermolysis and prevent heavy oil from charring.[29] The viscosity of heavy oil can be greatly reduced even by an order of magnitude or more when acid gases, such as CO_2 and H_2S, are dissolved in the heavy oil,[30-32] and the role of CO_2 in the aquathermolysis reaction has been further discussed by combined characterization methods. Particularly, the C–S bond energy is lowest in the heavy oil, and it is believed that the C–S bond cleavage of the sulfur-containing organic compounds in heavy oil is the main cause of H_2S generation.[33] On this basis, H_2S generation was used to represent the extent of the aquathermolysis reaction.

To clarify the influence of superheated steam on aquathermolysis, H_2S generation at different superheat degrees was

Table 3 Gas products obtained under different degrees of superheat ($mL\ g^{-1}$ oil)

Products	Superheat degrees (°C)			
	23.45	35.88	45.41	49.54
CH_4	2.250	4.017	9.055	14.784
C_2H_6	2.133	4.510	8.176	15.916
C_2H_4	11.309	14.399	11.357	18.043
C_3H_8	0.000	0.000	0.000	0.000
C_3H_6	0.000	0.000	0.000	0.000
i-C_4H_{10}	24.044	14.417	12.480	22.433
n-C_4H_{10}	3.076	19.557	2.662	0.660
n-C_4H_8	10.837	7.630	9.455	1.879
i-C_5H_{12}	0.000	0.000	0.000	0.202
n-C_5H_{12}	0.000	3.004	15.595	1.277
C6+	2.161	2.981	7.598	13.924
H_2	0.236	0.185	0.185	0.147
CO	0.000	0.000	0.000	0.000
CO_2	0.392	0.438	0.368	0.362
H_2S	0.0016	0.031	0.053	0.078
Olefins	22.146	22.030	20.812	19.922
Alkane	31.503	45.505	47.969	55.273

explored, as shown in Fig. 2. The results agreed well with the previous conclusion that the H_2S generation increased with the increasing reaction temperature.[22] This indicates that H_2S generation increased with an increase in the superheat degree even at the same reaction temperature. For example, when the reaction temperature was 300 °C, the H_2S generation increased from 0.178 to 0.345 mL g^{-1} oil with an increase in the superheat degree from 62.19 to 89.42 °C. Furthermore, the change in H_2S generation was more significant under higher temperature conditions even with a similar magnitude of change in the superheat degree. Higher superheat degree led to changes in the physicochemical properties of steam. The H_2S generation was promoted by the increase in the dielectric constant, solubility, and acidity and alkalinity.[34,35] In addition, the intermolecular forces and the hydrogen bonding forces were reduced at high superheat degrees. The conjugated large π bonds in the heavy oil structure, the side chain of the aromatic ring, and the C–S, C–O, and C–N bonds in the branches easily broke, leading to ring-opening, desulfurization, hydrogenation and dechaining reactions.

3.2 Transformation among SARA

The abovementioned compositions of the gas products indicate the complexity of the aquathermolysis reaction. Similarly, this complexity can also be reflected by the transformation among heavy oil fractions after reactions. Both the crude oil and the residual oil were separated into SARA, and the corresponding results at the temperature of 250 °C are shown as an example in Fig. 3.

Compared with the case of the crude oil, the saturate, aromatic and asphaltene fractions increased significantly, whereas the resin fraction decreased with the increasing superheat degree in the residual oil. Some free radicals were formed by molecular bond cleavage during the aquathermolysis reaction. These radicals could break macromolecular hydrocarbons to form small molecular saturated hydrocarbons, resulting in an increase in the saturate and aromatic fractions. With the increasing superheat degree, the intermolecular and
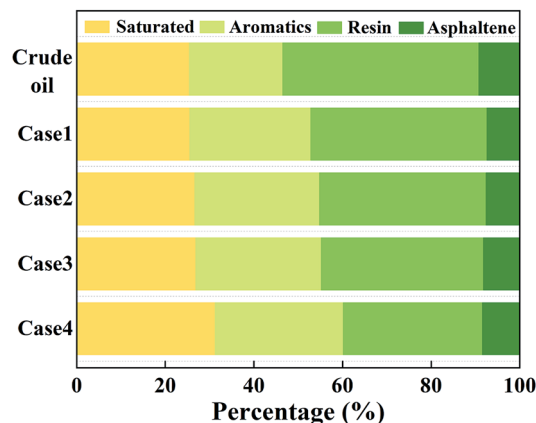
Fig. 3 Percentage of SARA at different superheat degrees.

hydrogen bonding forces weakened. Consequently, the aromatic ring structure and its branched C–S and C–O were more easily broken to form more free radicals.[36] These radicals can induce polycondensation to form asphaltene. In addition, sulfidation is another reason for the simultaneous formation of asphalt and H_2S.[37]

In addition to the overall analysis of SARA, the elemental content was detected to identify the primary source of H_2S generation. The S and H element contents at different superheat degrees are displayed in Fig. 4a and b, respectively. As can be observed from Fig. 4a, the content of S in all the fractions decreases as the superheat degree increases, indicating that all organic sulfur species contribute to the generation of H_2S. However, the specific contribution varied from one fraction to another. Particularly, the S element in saturate could not even be detected after all the reactions. The H element in water may participate in the reactions of H_2S generation, and it can be observed from Fig. 4b that the H element in the saturate fraction increases significantly. In addition, the sulfur content was more highly concentrated in the aromatic fraction according to the elemental analysis of crude oil. Fig. 4a suggests that the content of the S element in the aromatic fraction presents largest reduction with the increasing superheat degree. Therefore, organic sulfur in the saturate and aromatic fractions may be the main source of H_2S generation.

3.3 Oil product characterization

3.3.1 FTIR analysis.
To determine the structural changes in heavy oil after the reaction, FTIR detection in the range of 500–4000 cm^{-1} was performed, and the results obtained at different superheat degrees are shown in Fig. 5. All spectra contained similar absorption bands. The strong peaks at 2924 and 2854 cm^{-1} represented the asymmetric and symmetric stretching of the C–H bond of the methylene groups, respectively.[38,39] The absorption peaks at 1458 and 1378 cm^{-1} were attributed to the symmetric bending of the methyl groups,[40] suggesting that large amounts of aliphatic alkyl groups were present in the residual oil. The breakdown of naphthenic
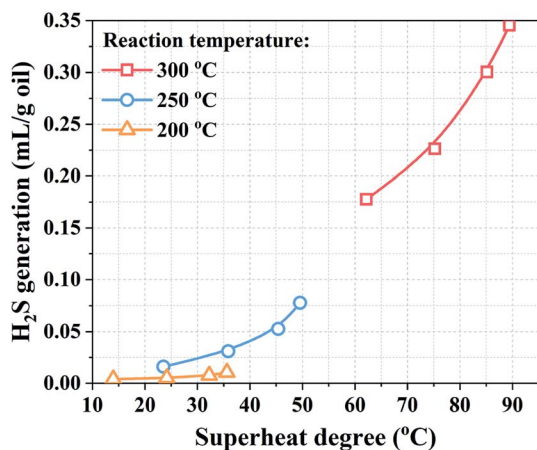
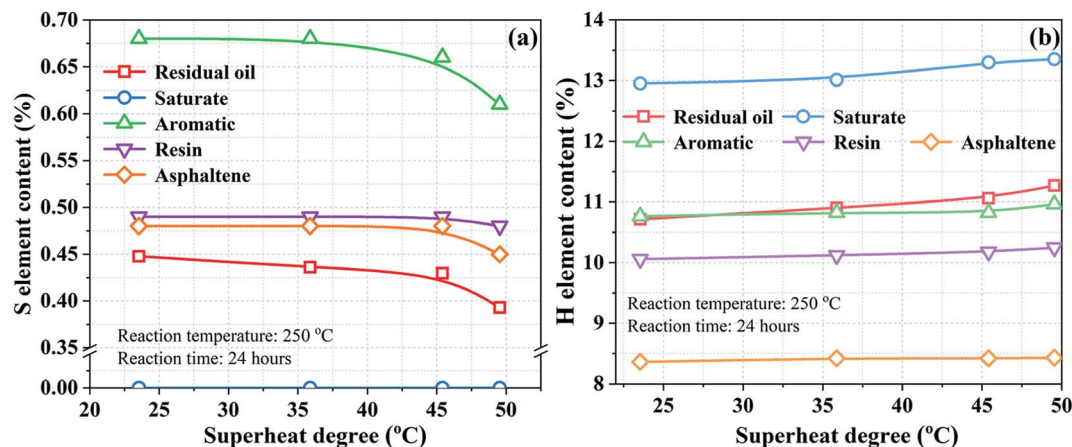Fig. 2 H_2S generation at different temperatures and superheat degrees.

Fig. 4 (a) S element and (b) H element contents at different superheat degrees.
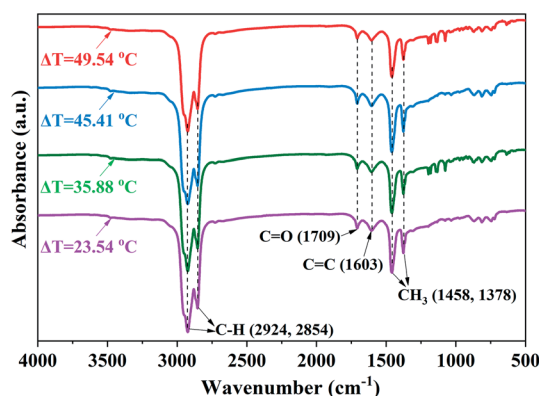

Fig. 5 FTIR spectra of heavy oil at different superheat degrees ($T = 250\ °C$).

bridges in these groups may lead to the reduction of the S content in heavy oils.[41] In addition, as the superheat degree increased, the FTIR spectra displayed a small decrease in the intensity near the peak 1709 cm^{-1}, which was related to the C=O stretching of the carbonyl and/or carboxyl groups.[42] Moreover, with the increasing superheat degrees, the FTIR spectra exhibited almost no change in the range of 2000–2300 cm^{-1}; this indicated that heavy oil contained almost no C≡C and C≡N.[43]

3.3.2 XPS analysis. To characterize the existing forms of heteroatoms in heavy oil, the XPS analysis was conducted, and the fitting curves of the C1s, O1s, N1s and S2p peaks for the oil obtained after the reaction at 250 °C are presented in Fig. 6.

The peaks at 284.70 and 285.22 eV represented the aliphatic and aromatic carbons combined with oxygen atoms, respectively. The connection modes of the carbon and oxygen atoms can be further classified into three kinds. The peaks at 531.50, 532.36 and 533.26 eV correspond to the carbons combined with the oxygen atoms *via* ethers and hydroxyls, carbonyl, and carboxyl.[44] The existing forms of nitrogen and sulfur in the heavy oil can also be detected by XPS. The N1s spectra mainly consisted of pyrrolic, pyridine, quaternary and chemisorbed

NO_x corresponding to the peaks at 398.78, 399.47, 400.00 and 400.60 eV.[45] Similarly, the peaks at 163.70, 164.46, 165.50, 168.07, and 168.96 eV in the S2p spectra can be categorized into the peaks of sulfides, thiophenes, sulfoxides, sulfones, and acids/sulfates, respectively.

The XPS results of the organic C, O, N, and S forms in heavy oil before and after the reaction are summarized in Table 4. As can be seen, the heavy oil is mainly composed of aliphatic and aromatic compounds. Compared to the case of the oil before reaction, the number of the carbon–oxygen bonded atoms in the oil after the reaction was reduced; the number of the carbonyl and carboxyl groups was also relatively reduced, but that of the hydroxyl group increased. The carbonyl group was formed by the cleavage of the C–O bond in the carboxyl group. On this basis, gaseous CO_2 was produced from the carbonyl group, and the escaping CO_2 was detected in the gas products (Table 1).

H_2S generation was not only determined by the content of sulfur in heavy oil but also closely related to the chemical structure of sulfur-bearing molecules.[17] As can be seen from Table 4, the main existing forms of sulfur in the heavy oil after reaction are sulfoxide and thiophene, which account for 70.49% of the total sulfur. In general, sulfoxide is more stable than other sulfides. It can only be decomposed to produce H_2S when the reaction temperature exceeds 300 °C.[46] Therefore, a large amount of sulfoxide remained in the residual after the reaction. By comparing the sulfur-containing substances before and after the reaction, it was found that H_2S was mainly formed by sulfides, sulfones or sulfates under superheated steam conditions. Payzant *et al.*[47] believed that the depolymerization of macromolecules, such as colloidal and asphaltenes, also produced thiophenes. By combining the abovementioned findings with those of the SARA analysis, it can be further concluded that the increase in the content of thiophene at high superheat degrees is mainly caused by resin degradation. Although the sulfone and sulfate contents were low before and after the reaction, they were still detected, and both of them decreased after the reaction due to the thermochemical reduction reaction.
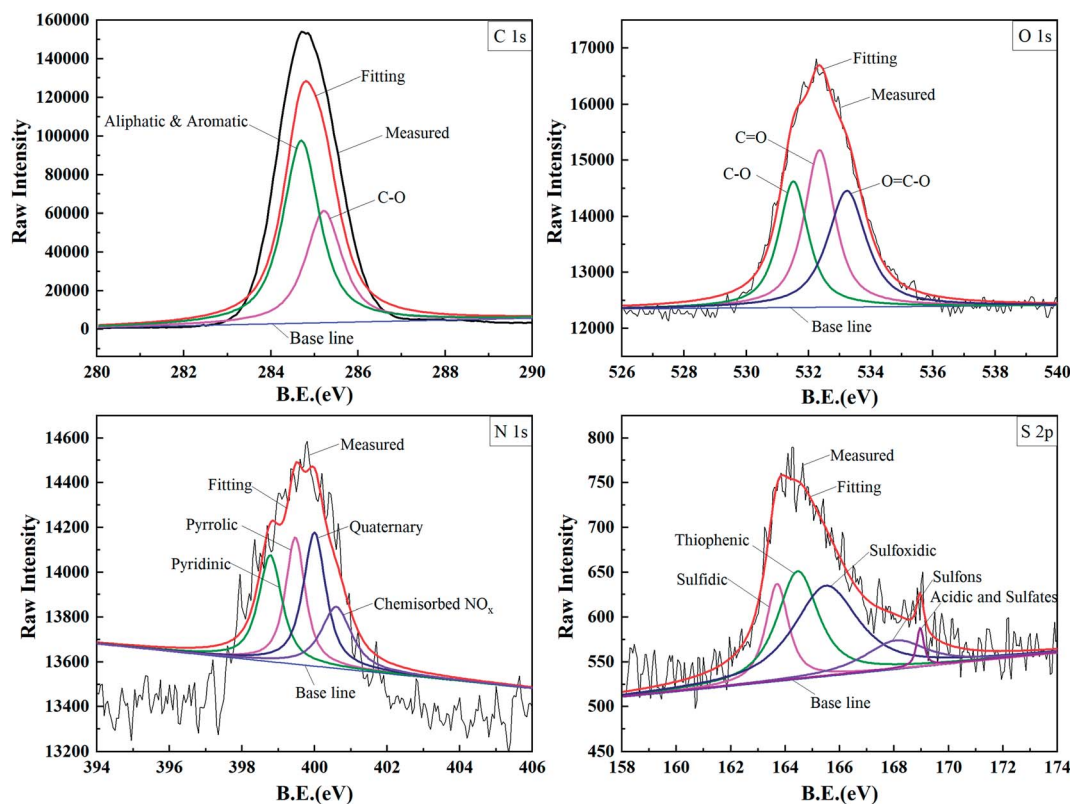
Fig. 6 XPS spectra of C1s, O1s, N1s and S2p and corresponding fitting curves for the oil obtained after the reaction at 250 °C (B.E., binding energy).

Table 4 XPS results of the organic C, O, N and S forms

Name	Group type	B.E. (eV)	FWHM (eV)	Relative peak area (%)	
				Before reaction	After reaction
C1s	C (al and ar)	284.70	1.00	62.22	62.11
	C joins to O	285.22	1.00	37.96	37.89
O1s	C=O	531.50	1.13	31.03	27.75
	C–O	532.36	1.21	33.92	39.48
	O=C–O	533.26	1.47	35.05	32.77
N1s	Pyrrolic	398.78	0.77	26.32	25.11
	Pyridinic	399.47	0.65	18.34	25.32
	Quaternary	400.00	0.75	27.80	30.67
	Chemisorbed NO_x	400.60	1.00	27.54	18.90
S2p	Sulfidic	163.70	1.00	19.71	15.25
	Thiophenic	164.46	1.81	19.80	30.48
	Sulfoxidic	165.50	2.84	19.94	40.01
	Sulfones	168.07	2.74	20.20	12.36
	Acidic/sulfates	168.96	0.50	20.34	1.90

4. Conclusions

The utilization of superheated steam is effective to promote H_2S generation. In this study, the effects of superheat degree on the H_2S generation during the simulated thermal enhanced oil recovery process were investigated. H_2S generation increased with an increase in the superheat degree at the same reaction temperature, and it increased to as high as 0.345 mL g^{-1} oil when the superheat degree increased to 89.42 °C.

Elemental analysis indicated that the sulfur-containing substances in the saturate and aromatic fractions were the main sources of H_2S generation. According to the FTIR analysis, the number of the methylene and methyl groups reduced with the increasing superheat degree. The main existing forms of sulfur in the heavy oil were characterized by the XPS analysis, and sulfur in the forms of sulfides, sulfones and sulfates was more likely to generate H_2S under superheated steam conditions.

Conflicts of interest

There are no conflicts of interest to declare.

Acknowledgements

References

1 P. Liu, Y. Wu and X. Li, *Fuel*, 2013, **111**, 12–19.
2 K. Guo, H. Li and Z. Yu, *Fuel*, 2016, **185**, 886–902.
3 A. Mohsenzadeh, Y. Al-Wahaibi, R. Al-Hajri, B. Jibril and N. Mosavat, *Fuel*, 2017, **187**, 417–428.
4 B. Hascakir, *J. Pet. Sci. Eng.*, 2016, **146**, 746–751.
5 F. J. Hein, *Nat. Resour. Res.*, 2006, **15**, 67–84.
6 D. W. Zhao, J. Wang and I. D. Gates, *Fuel*, 2014, **117**, 431–441.
7 P. D. Clark, J. B. Hyne and J. D. Tyrer, *Fuel*, 1984, **63**, 125–128.
8 G. Zhu, S. Zhang, H. Huang, Q. Liu, Z. Yang, J. Zhang, T. Wu and Y. Huang, *J. Pet. Sci. Eng.*, 2010, **71**, 30–36.
9 H. F. Thimm, *SPE Heavy Oil Conference-Canada*, Alberta, Canada, 2014.
10 P. D. Clark, J. B. Hyne and J. D. Tyrer, *Fuel*, 1983, **63**, 1649–1654.
11 J. Na, H. Zhao, Y. Tao, T. Ibatullin and J. Gao, *Energy Fuels*, 2016, **30**(7), 5291–5299.
12 W. Montgomery, R. W. Court, A. C. Rees and M. A. Sephton, *Fuel*, 2013, **113**, 426–434.
13 W. Montgomery, M. A. Sephton, J. S. Watson, H. Zeng and A. C. Rees, *Sci. Rep.*, 2015, **5**, 8159.
14 W. Montgomery, M. Sephton, J. Watson and H. Zeng, *SPE Heavy Oil Conference-Canada*, Alberta, Canada, 2014.
15 P. Zhao, C. Li, C. Wang and M. Yang, *Liq. Fuels Technol.*, 2016, **34**, 1452–1461.
16 C. Barroux and V. Lamoureux-Var, *SPE Heavy Oil Conference-Canada*, Alberta, Canada, 2013.
17 V. Lamoureux-Var and F. Lorant, *IOR 2005-13th European Symposium on Improved Oil Recovery*, Budapest, Hungary, 2005.
18 V. Lamoureux-Var, E. Kohler, A. Y. Huc, E. Berger and L. Fusetti, *Natural Gas Geochemistry: Recent Developments, Applications, and Technologies*, Orinoco Belt, Venezuela, 2011, pp. 9–12.
19 A. R. Katritzky and S. M. Allin, *Acc. Chem. Res.*, 1996, **29**, 399–406.
20 M. Siskin and A. R. Katritzky, *Chem. Rev.*, 2001, **101**, 825–836.
21 Y. V. Lysogorskiy, R. M. Aminova and D. A. Tayurskii, *AIP Conf. Proc.*, 2015, **1702**(1), 825–836.
22 R. Lin, D. Song, X. Wang and D. Yang, *Energy Fuels*, 2016, **30**, 5323–5329.
23 X.-Y. Duan, F.-B. Li, B. Ding, L. Gong and M.-H. Xu, *J. Therm. Anal. Calorim.*, 2019, DOI: 10.1007/s10973-019-08821-5.
24 F. Sun, Y. Yao, X. Li and L. Zhao, *Int. J. Heat Mass Transfer*, 2017, **113**, 850–860.
25 F. Sun, Y. Yao, M. Chen, X. Li, L. Zhao, Y. Meng, Z. Sun, T. Zhang and D. Feng, *Energy*, 2017, **125**, 795–804.
26 F. Sun, Y. Yao, X. Li, G. Li and Z. Sun, *Int. J. Heat Mass Transfer*, 2018, **121**, 282–289.
27 S. Zhang, J. Mi and K. He, *Chem. Geol.*, 2013, **349**, 27–35.
28 A. Xu, L. Mu, Z. Fan, X. Wu, Z. Lun, B. Bing and T. Xu, *J. Pet. Sci. Eng.*, 2013, **111**, 197–207.
29 H. Kawai and F. Kumata, *Catal. Today*, 1998, **43**, 281–289.
30 H. Li, S. Zheng and D. T. Yang, *SPE J.*, 2013, **18**, 695–707.
31 A. K. M. Jamaluddin, D. B. Bennion, F. B. Thomas and M. A. Clark, *Abu Dhabi International Petroleum Exhibition & Conference*, Abu Dhabi, 1998.
32 A. Fayazi and A. Kantzas, *Rev. Chem. Eng.*, 2019, **35**, 393–419.
33 Y. Hamedi Shokrlu and T. Babadagli, *SPE Reservoir Eval. Eng.*, 2013, **16**, 333–344.
34 Y. V. Lysogorskiy, R. M. Aminova and D. A. Tayurskii, *AIP Conf. Proc.*, 2015, **1702**(1), 825–836.
35 T. J. Houser, D. M. Tiffany, Z. Li, M. E. Mccarville and M. E. Houghton, *Fuel*, 1986, **65**, 827–832.
36 Y. Chen, Y. Wang, C. Wu and X. Fei, *Energy Fuels*, 2008, **22**, 1502–1508.
37 I. Kowalewski, P. Schaeffer, P. Adam, D. Dessort, A. Fafet and B. Carpentier, *Org. Geochem.*, 2010, **41**, 951–958.
38 B. Hazra, A. K. Varma, A. K. Bandopadhyay, S. Chakravarty, J. Buragohain, S. K. Samad and A. K. Prasad, *J. Nat. Gas Sci. Eng.*, 2016, **32**, 239–255.
39 Y. Chen, A. Furmann, M. Mastalerz and A. Schimmelmann, *Fuel*, 2014, **116**, 538–549.
40 J. Shi, Y. Ma, S. Li and L. Zhang, *Energy Fuels*, 2017, **31**, 10535–10544.
41 C. Wu, L. Huo, C. Yao, B. Cao and X. Li, *Spec. Oil Gas Reservoirs*, 2011, **18**, 101–104.
42 I. Z. Rakhmatullin, S. V. Efimov, V. A. Tyurin, A. A. Al-Muntaser, A. E. Klimovitskii, M. A. Varfolomeev and V. V. Klochkov, *J. Pet. Sci. Eng.*, 2018, **168**, 256–262.
43 J. Taheri-Shakib, A. Shekarifard and H. Naderi, *Fuel*, 2018, **228**, 243–253.
44 T. Tunstall, *Energy*, 2015, **93**, 580–588.
45 J. Friebel and R. F. W. Köpsel, *Fuel*, 1999, **78**, 923–932.
46 S. Jian, M. Yue, S. Li and Z. Lei, *Energy Fuels*, 2017, **31**(10), 10535–10544.
47 J. Payzant, D. McIntyre, T. Mojelsky, M. Torres, D. Montgomery and O. Strausz, *Org. Geochem.*, 1989, **14**, 461–473.